

# USED FUEL DISPOSITION CAMPAIGN

## *Coupling the Mixed Potential and Radiolysis Models for Used Fuel Degradation*

**Fuel Cycle Research & Development**

*Prepared for  
U.S. Department of Energy  
Used Fuel Disposition  
Campaign*

*Edgar C. Buck  
James L. Jerden, Jr.  
William L. Ebert  
Richard S. Wittman*

*August 30, 2013*

PNNL-22701

FCRD-UFD-2013-000290

M3FT-PN0806058



Disclaimer

This information was prepared as an account of work sponsored by an agency of the U.S. Government. Neither the U.S. Government nor any agency thereof, nor any of their employees, makes any warranty, expressed or implied, or assumes any legal liability or responsibility for the accuracy, completeness, or usefulness, of any information, apparatus, product, or process disclosed or represents that its use would not infringe privately owned rights. References herein to any specific commercial product, process, or service by trade name, trade mark, manufacturer, or otherwise, does not necessarily constitute or imply its endorsement, recommendation, or favoring by the U.S. Government or any agency thereof. The views and opinions of the authors expressed herein do not necessarily state or reflect those of the U.S. Government or any agency thereof.

**Peer Review:**

---

David Sassani  
Sandia National Laboratories

**Concurrence:**

---

Kevin McMahon (Sandia National Laboratories)  
Used Fuel Disposition Control Account Manager

**Submitted by:**

*Edgar C. Buck*

---

Edgar C. Buck  
Pacific Northwest National Laboratory

## EXECUTIVE SUMMARY

This report fulfills the M3 milestone M3FT-PN0806058.

The primary purpose of this report is to describe the strategy for coupling three process level models to produce an integrated Used Fuel Degradation Model (FDM). The FDM, which is based on fundamental chemical and physical principals, provides direct calculation of radionuclide source terms for use in repository performance assessments.

The G-value for  $\text{H}_2\text{O}_2$  production ( $G_{\text{cond}}$ ) to be used in the Mixed Potential Model (MPM) ( $\text{H}_2\text{O}_2$  is the only radiolytic product presently included but others will be added as appropriate) needs to account for intermediate spur reactions. The effects of these intermediate reactions on  $[\text{H}_2\text{O}_2]$  are accounted for in the Radiolysis Model (RM). This report details methods for applying RM calculations that encompass the effects of these fast interactions on  $[\text{H}_2\text{O}_2]$  as the solution composition evolves during successive MPM iterations and then represent the steady-state  $[\text{H}_2\text{O}_2]$  in terms of an “effective instantaneous or conditional” generation value ( $G_{\text{cond}}$ ). It is anticipated that the value of  $G_{\text{cond}}$  will change slowly as the reaction progresses through several iterations of the MPM as changes in the nature of fuel surface occur. The  $G_{\text{cond}}$  values will be calculated with the RM either after several iterations or when concentrations of key reactants reach threshold values determined from previous sensitivity runs. Sensitivity runs with RM indicate significant changes in G-value can occur over narrow composition ranges.

The objective of the mixed potential model (MPM) is to calculate the used fuel degradation rates for a wide range of disposal environments to provide the source term radionuclide release rates for generic repository concepts. The fuel degradation rate is calculated for chemical and oxidative dissolution mechanisms using mixed potential theory to account for all relevant redox reactions at the fuel surface, including those involving oxidants produced by solution radiolysis and provided by the radiolysis model (RM). The RM calculates the concentration of species generated at any specific time and location from the surface of the fuel.

Several options being considered for coupling the RM and MPM are described in the report. Different options have advantages and disadvantages based on the extent of coding that would be required and the ease of use of the final product.

## CONTENTS

EXECUTIVE SUMMARY .....	iv
CONTENTS.....	v
ACRONYMS.....	vi
1. INTRODUCTION.....	1
2. SUMMARY OF RADIOLYSIS MODEL .....	2
2.1 Objective .....	2
2.2 Physical Model.....	2
2.3 Mathematical model.....	4
2.3.1 Geometric scale.....	5
2.3.2 Time scale .....	6
3. SUMMARY OF MIXED POTENTIAL MODEL .....	8
3.1 Objective and Background.....	8
3.2 Physical model .....	9
3.3 Mathematical Model .....	12
3.3.1 Geometric Scale .....	13
3.3.2 Time Scale .....	14
3.4 Example of MPM Calculations.....	14
4. COUPLING MPM/RM MODELS .....	16
4.1 Parameter values provided by RM to MPM.....	17
4.2 Parameter values provided by MPM to RM.....	18
4.3 Interface Approaches .....	19
5. Conclusions .....	21
6. References .....	23

## ACRONYMS

ANL	Argonne National Laboratory
DOE-NE	U.S. Department of Energy Office of Nuclear Energy
EBS	Engineered Barrier System
FACSIMILE	Commercial computational code for determining radiolytic species
FDM	Fuel Degradation Model
Gy	Gray (radiation dose)
GWd/MTU	Giga-Watt days per metric tonne uranium metal
IRF	Instant Release Fraction
IRM	Instantaneous Release Model
MAKSIMA-CHEMIST	Code to compute the kinetics of simultaneous chemical reactions
MPM	Mixed Potential Model
PNNL	Pacific Northwest National Laboratory
PA	Performance Assessment
rad/s	radiation dose per second
RM	Radiolysis Model
SNL	Sandia National Laboratories
UNF	used nuclear fuel

## 1. INTRODUCTION

The primary purpose of this report is to describe the strategy for coupling three process level models to produce an integrated Used Fuel Degradation Model (FDM). The FDM, which is based on fundamental chemical and physical principals, provides direct calculation of radionuclide source terms for use in repository performance assessments. The matrix degradation model is used to calculate  $UO_2$  degradation rates by chemical and oxidative dissolution mechanism based on electrochemical theory in the mixed potential model (MPM) (Jerden et al. 2013). The radiolysis model (RM) is used to calculate steady state concentrations of radiolytic species (Wittman and Buck, 2012) that participate in redox reactions modeled in the matrix degradation model. The FDM source term includes radionuclides released from gap and grain boundaries as quantified using an instantaneous release model (IRM) (Sassani et al. 2012). The programmatic context for the work described in this report is shown in Figure 1.1. The FDM uses input properties of the fuel waste forms and disposal environment to calculate the rate of fuel degradation as the conditions at the fuel surface evolve over time. Radionuclides in the fuel are mobilized at the same rate and made available for transport away from the waste package. The FDM model provides the source term concentrations for radionuclides used in reactive transport models of the disposal system.

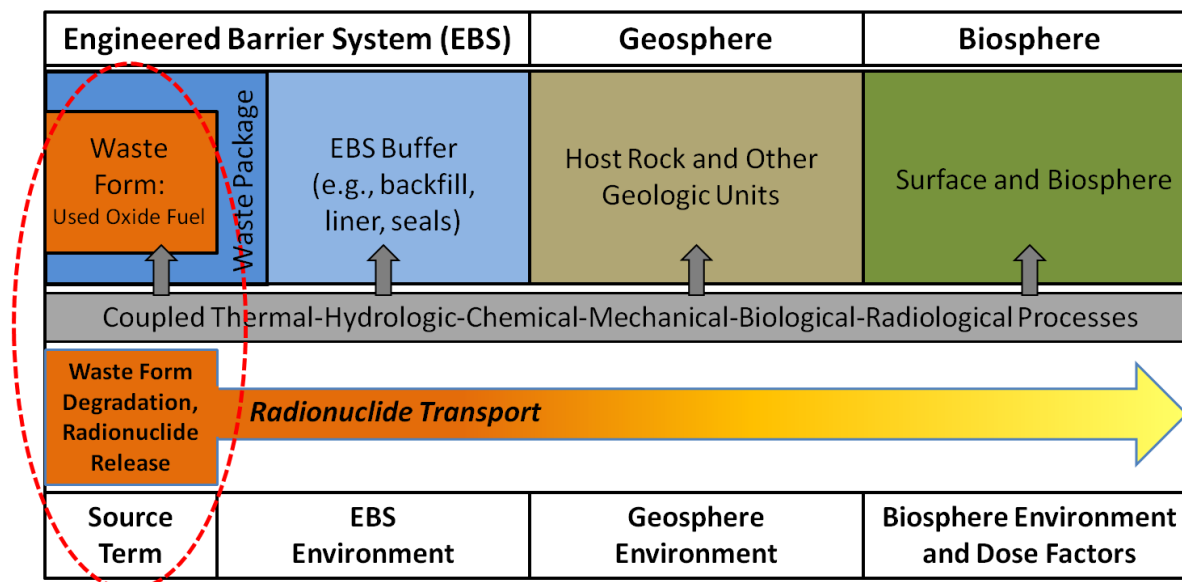


**Figure 1.1** Components of a generic disposal system for used oxide fuel (adapted from Freeze et al. 2010). The red circle identifies the processes covered by the models described in this report.

## 2. SUMMARY OF RADIOLYSIS MODEL

The radiolysis model (RM) calculates the concentration of species generated at any specific time and location from the surface of the fuel (Wittman and Buck, 2012). The model will be used as a component in a total system model for assessing the performance of UNF in a geological repository. The total system model will account for time-dependent phenomena that may influence UNF behavior. One major difference between used fuel and natural analogues, including unirradiated  $\text{UO}_2$ , is the intense radiolytic field. The radiation emitted by used fuel can produce radiolysis products in the presence of water vapor or a thin-film of water (including hydroxide ( $\bullet\text{OH}$ ) and hydrogen ( $\bullet\text{H}$ ) radicals, oxygen ion ( $\text{O}_2^-$ ), aqueous electron ( $e_{\text{aq}}$ ), hydrogen peroxide ( $\text{H}_2\text{O}_2$ ), hydrogen gas ( $\text{H}_2$ ), and the secondary radiolysis product, oxygen ( $\text{O}_2$ )) that may increase the waste form degradation rate and change radionuclide behavior.

### 2.1 Objective

The radiolysis model developed for this analysis is formulated as a set of coupled kinetics equations for the reactions of aqueous species assumed to exist in the environment inside the Engineered Barrier System (EBS). Radiolytic species are generated at a rate that is based on the dose rate induced by the radiation field. Subsequent reactions of the radiolytic species are then computed based on the reaction kinetics. The model inputs are the reaction rate constants, the temperature and dose rate, the radiolytic G-values, and the initial concentrations of species in the system. The conditional G-value for  $\text{H}_2\text{O}_2$  production, ( $G_{i,\text{cond}}$ ), is provided to the MPM (see equation 2.3).

### 2.2 Physical Model

It is well known that the radiation emitted by used fuel will produce radiolysis products in the presence of water vapor or a thin-film of water (including  $\text{OH}\bullet$  and  $\text{H}\bullet$  radicals,  $\text{O}_2$ ,  $e_{\text{aq}}$ ,  $\text{H}_2\text{O}_2$ ,  $\text{H}_2$ , and  $\text{O}_2$ ). However, for these products to increase or change the rate of UNF degradation and result in the release of radionuclides requires understanding the processes that might occur in these interfacial regions.

The initial attempts of radiolysis model development concerned the production of radiolytic species with time. Developing codes that would provide values for time periods relevant to experimentation required modifying codes for stability. Diffusional terms were added to provide greater realism in the model. This enabled determination of a 'steady state' value for a particular radiolytic species or other chemical species distant from the fuel surface. These are the values that would be provided to the MPM. A further improvement to the model has been to capture the dose dependent radiolytic processes that would occur very close to the surface. This adaptation has made the RM more closely related to the MPM. The earlier versions assumed almost constant dose within the first 30  $\mu\text{m}$  of the surface where most alpha energy would be deposited. However, it was realized that this was a poor representation of the system and this region was further sub-divided into zones where the dose was modeled to change with distance

from the surface. The radiolysis model remains effectively a one-dimensional model of the surface of the fuel.

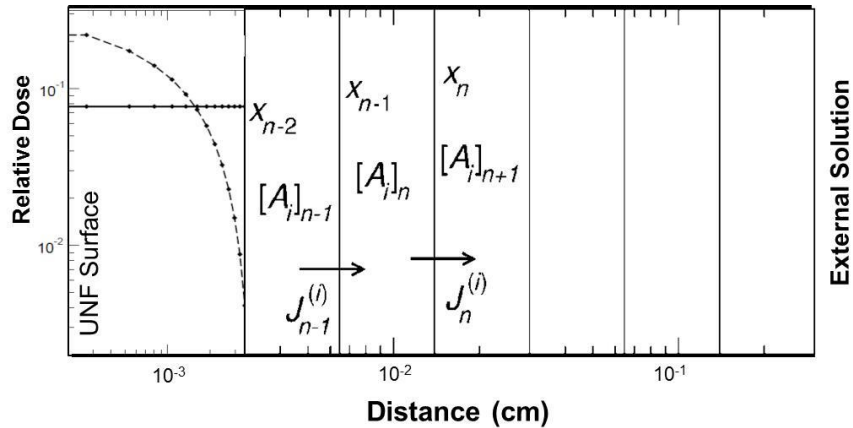


**Figure 2.1** Radiolysis model showing generation modified with a dose dependence term in the irradiated zone and the diffusion zones across spatial regions.

The early versions of the radiolysis model were verified by using the reactions reported by Pastina and LaVerne (2001) and those of Poinssot et al. (2005) to reproduce their results, which had been done using FACSIMILE and MAKSIMA-CHEMIST kinetic software products, respectively.

**Table 2.1** Alpha particle G-values (Pastina and LaVerne, 2001)

<i>Species</i>	<i>G-value at 5 MeV (molecules/100-eV)</i>
H <sup>+</sup>	0.18
H <sub>2</sub> O	-2.58
H <sub>2</sub> O <sub>2</sub>	1.00
e <sub>(aq)</sub>	0.15
•H	0.10
•OH	0.35
•HO <sub>2</sub>	0.10
H <sub>2</sub>	1.20

### User-defined inputs

- Length of model diffusion grid (fuel surface to environmental boundary, default is 5 millimeters)
- Number of calculation nodes (points) in diffusion grid (default is 24) with 14 zones in the alpha penetration zone.
- Duration of simulation (days to reach steady state)

## Parameters

- Alpha-particle penetration depth (35  $\mu\text{m}$ )
- Generation value for  $\text{H}_2\text{O}_2$  ( $G_{\text{H}_2\text{O}_2}$ ) (moles per alpha energy deposited per time) (see Table 1 for  $\text{H}_2\text{O}_2$  and other species)
- Rate constants (*function of temperature*) (taken from Pastina and LaVerne, 2001; Poinssot et al. 2005)
- Diffusion coefficients (*function of temperature*) (see Table 2)
- Activation energies for temperature dependencies (available for  $\text{H}_2\text{O}_2$  only)

## Constants (not explicit in model)

- pH of bulk solution (case dependent)
- Pressure ( $\text{O}_2$ ,  $\text{H}_2$  are set and tracked as dissolved concentrations)

## Variables

- Dose rate
- Temperature
- Starting concentrations of oxidants and complexants:  $[\text{O}_2]$ ,  $[\text{CO}_3^{2-}]$ ,  $[\text{H}_2]$

## Calculated by model (output)

- Conditional G-value for  $\text{H}_2\text{O}_2$
- Conditional G-values for all other species (not used in MPM)

## 2.3 Mathematical model

Concentrations in each region are coupled through diffusive currents and are expressed in Equations 2.1 and 2.2. The coupled kinetics rate equations for the solution species concentrations  $[A_i]$  are:

$$\frac{d[A_i]_n}{dt} + \frac{J_n^{(i)} - J_{n-1}^{(i)}}{x_n - x_{n-1}} = G_i \dot{d}_n + \sum_{r=1}^{N_r} k_{ir} \prod_{j_r=1}^{n_r} [A_{j_r}]_n^{O_{j_r}} \quad (2.1)$$

with rate constants  $k_{ir}$ , dose rate and radiolytic generation constants  $G_i$ , where the diffusive currents ( $J^{(i)}$ ) and diffusion constants ( $D_i$ ) appear in the discretized Fick's Law according to:

$$J_n^{(i)} = -2D_i \frac{[A_i]_{n+1} - [A_i]_n}{x_{n+1} - x_{n-1}} \quad (2.2)$$

for each component  $i$  in region  $n$ . Table 2 shows the values of diffusion constants used in the model. For brevity, the “sum-of-products” on right-hand side of Equation 2.1 expresses the sum of the product of reactant concentrations entering with reaction order  $O_{jr}$  where the multiplication-index  $j_r$  is over the  $n_r$  reactants for reaction  $r$ . The notation includes the final state order of component  $i$  produced by writing the rate constants  $k_{ir}$ , dependent on index  $i$ , but of course that dependence only amounts to an integer (which could be zero) multiplied by the reaction rate constants.

**Table 2.2** Diffusion constants (Christensen and Sunder, 1996)

Species	$D_i (10^{-5} \cdot \text{cm}^2 \cdot \text{s}^{-1})$
$e_{(\text{aq})}^-$	4.9
OH	2.3
$O^-$	1.5
$H_2O_2$	1.9
$O_2$	2.5
$H_2$	6.0
Others	1.5

### 2.3.1 Geometric scale

The length of the logarithmic grid of the model diffusion cell is adjustable but was set at 3 millimeters for all of the sensitivity runs performed to date (Figure 2.2). The number of calculation points along the diffusion grid can also be set by the user but has been adjusted to match the MPM.

We consider only the  $\alpha$ -induced G-values (Table 2.1) because the near-field dose at the fuel surface is strongly dominated by  $\alpha$ -dose for decay times greater than 30 years when the dose is  $\sim 160$  rad/s for 50 GWd/MTU used nuclear fuel (Radulescu, 2011). Consistent with  $\alpha$ -decay radiation, the dose rate is assumed to be nonzero only in the nearest 35  $\mu\text{m}$  to the fuel surface. Figure 2.1 shows the spatial regions modeled from near the fuel surface to the external solution boundary considered to be at 3.5 mm. The products of G-values with the dose rate act as generation term to the kinetics equations for each of the species and are represented in Figure 2.2. Concentrations in each region are coupled through diffusive currents and are expressed in Equations 2.1 and 2.2. Within the first 35  $\mu\text{m}$  layer, the radiation dose will be greatest immediately close to the fuel surface and then drop off. The radiolysis model can either consider a constant average dose in this region, or consider the dose dependent production of radiolytic species. In Figure 2.2, the effect of including or excluding dose dependence is shown.

When the dose dependence is included,  $H_2O_2$  production close to the fuel surface decreases. The conditional G-value ( $G_{i,cond}$ ), is calculated from Equation 2.3 (see below) for each node within the alpha penetration zone :

$$\bar{G}_{i,\text{cond}} \equiv G_i + \frac{1}{x_d \rho \dot{d}} \int_0^{x_d} dx \left\{ \sum_{r=1}^{N_r} k_{ir} \prod_{j_r=1}^{n_r} [A_{j_r}]^{O_{j_r}} \right\}_{\text{Steady-State}} = \frac{1}{\rho \dot{d}} \left\{ \frac{J^{(i)}(x_d)}{x_d} \right\}_{\text{Steady-State}} \quad (2.3)$$

where  $\rho$  is the density,  $\dot{d}$ , is the dose rate, and  $x_d$  is the radiation zone distance.

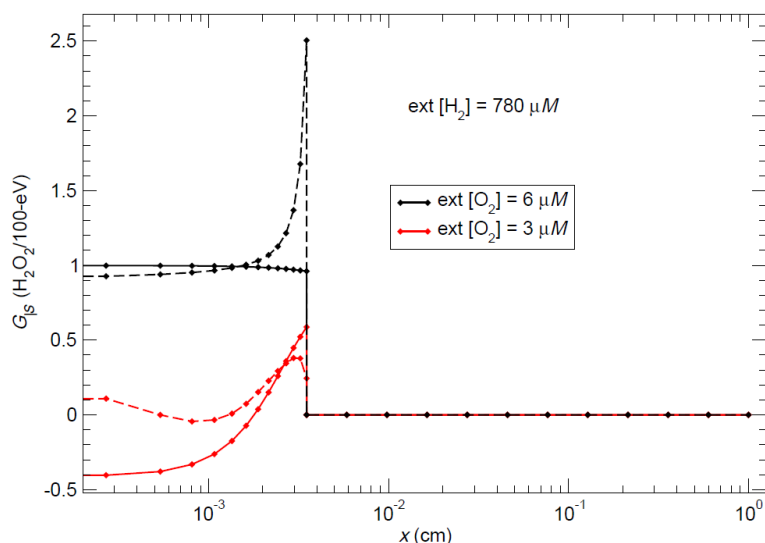


**Figure 2.2** Predicted conditional G-values for  $\text{H}_2\text{O}_2$  with distance from the fuel surface showing effect of external  $\text{O}_2$  at a fixed  $\text{H}_2$  concentration.

### 2.3.2 Time scale

The magnitude of each time step is determined by the total simulation time and the number of temporal calculation points specified. Both of these values are set by the user. The time steps are spaced logarithmically, with the finer spacing at the beginning of the run. For simulation runs of 1-10 days, optimal time steps range from 0.1 seconds early in the simulation to hours towards the end of the simulation.

The kinetics equations become unceasingly stiff as a dose rate of 137~rad/s is approached from below (Figure 2.3). At a dose rate of 138 rad/s, the solution transitions to a new steady state which is smaller in the  $\text{H}_2\text{O}_2$  and  $\text{O}_2$  concentrations - even though the dose rate is greater. The steady state solution is non-unique for this system. This is not surprising because of the many non-linear terms in the kinetics equations. Additionally, at least two steady state solutions exist above and below the critical dose rate, but only one is attained for a specific initial condition. The dashed curves in Figure 2.4 assume that the dose rate changes continuously after the previous steady state is attained in both the forward (red-dashed) and reverse (black-dashed)

direction. The dose change in the reverse (black-dashed) direction shows that two steady state solutions exist even below the critical dose rate.

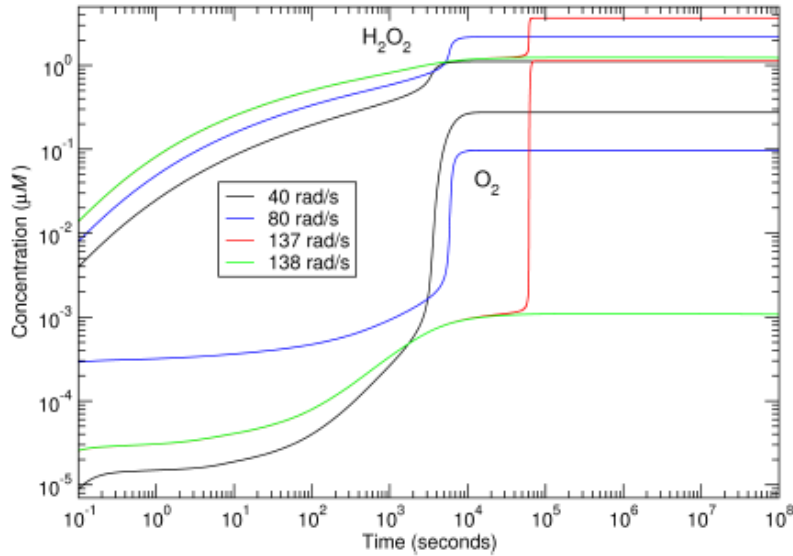


**Figure 2.3** Time dependent concentration of H<sub>2</sub>O<sub>2</sub> and O<sub>2</sub> at the surface with dose rates of 40 rad/s (black), 80 rad/s (blue), 137 rad/s (red), 138 rad/s (green).

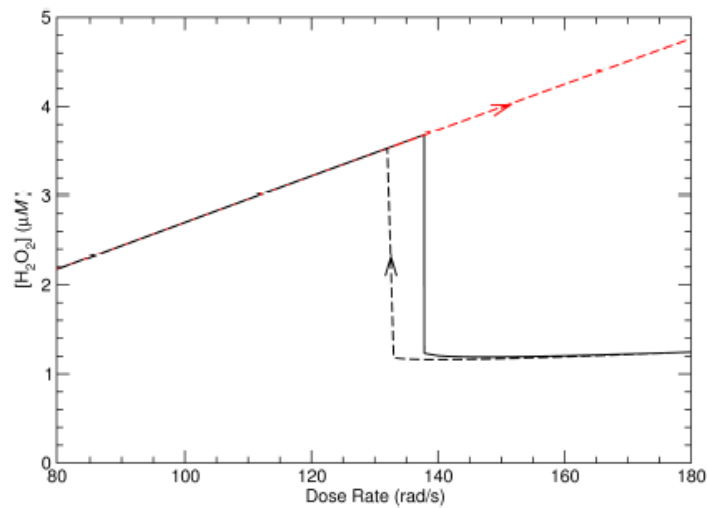


**Figure 2.4** Steady-state concentrations of H<sub>2</sub>O<sub>2</sub> at surface with dose rate for fixed initial conditions (black-solid), forward running steady-stated (red-dashed), reverse running steady-state (black-dashed).

Results from the radiolysis model including diffusional terms, suggests that steady state conditions under two conditions can lead to discrete jumps in concentrations. It has been observed, even at fixed dose rate that jumps in conditional G-values can occur.

### 3. SUMMARY OF MIXED POTENTIAL MODEL

#### 3.1 Objective and Background

The objective of the mixed potential model (MPM) is to calculate the used fuel degradation rates for a wide range of disposal environments to provide the source term radionuclide release rates for generic repository concepts. The fuel degradation rate is calculated for chemical and oxidative dissolution mechanisms using mixed potential theory to account for all relevant redox reactions at the fuel surface, including those involving oxidants produced by solution radiolysis. The MPM was developed to account for the following key phenomena (Jerden et al. 2013):

- Rate of oxidative dissolution of the fuel matrix as determined by interfacial redox reaction kinetics (quantified as corrosion potential) occurring at the multiphase fuel surface (phases include  $\text{UO}_2$  and the fission product alloy or epsilon phase).
- Chemical or solubility based dissolution of the fuel matrix.
- Complexation of dissolved uranium by carbonate near the fuel surface and in the bulk solution.
- Production of hydrogen peroxide (the dominant fuel oxidant in anoxic repository environments) by alpha-radiolysis.
- Diffusion of reactants and products in the groundwater away from and towards the reacting fuel surface.
- Precipitation and dissolution of a U-bearing corrosion product layer on the fuel surface.
- Diffusion of reactants and products through the porous and tortuous corrosion layer covering the reacting fuel surface.
- Arrhenius-type temperature dependence for all interfacial and bulk reactions.

Because the MPM is based on fundamental chemical and electrochemical principles, it is flexible enough to be applied to the full range of repository environments as well as shorter-term storage scenarios being considered as part of the UFD campaign. The Argonne Mixed Potential Model (MPM) was produced by implementing the Canadian mixed potential model for  $\text{UO}_2$  fuel dissolution (King and Kolar, 1999, King and Kolar, 2003, Shoesmith et.al., 2003) using the numerical computing environment and programming language MATLAB. The implementation and testing of the Argonne MPM is discussed in the following reports: Jerden et al., 2012, FCRD-UFD-2012-000169 and Jerden et al., 2013 FCRD-UFD-2013-000057 and the integration of the MPM and RM with other process models being developed as part of the UFD program was discussed in Sassani et al., 2012, M2FT-12SN0806062. The MPM includes a simplified module for calculating the production of  $\text{H}_2\text{O}_2$ , which is the sole radiolytic species required in the current implementation for granitic environments. This is being replaced by the RM to take into account local variations in the concentrations of radiolytic species as affected by dose, chemical interactions in the groundwater, decay, and diffusion. Key aspects of the MPM

affecting the integration of the RM, including the geometric and temporal scales of the models, are discussed below.

### 3.2 Physical model

The MPM consists of ten one-dimensional reaction-diffusion equations (see Jerden et al., 2013), that describe the mass transport, precipitation/dissolution and redox processes of the ten chemical species included in the model. Figure 3.1 shows the MPM spatial diffusion grid and the distribution of individual calculation nodes (shown as vertical lines).

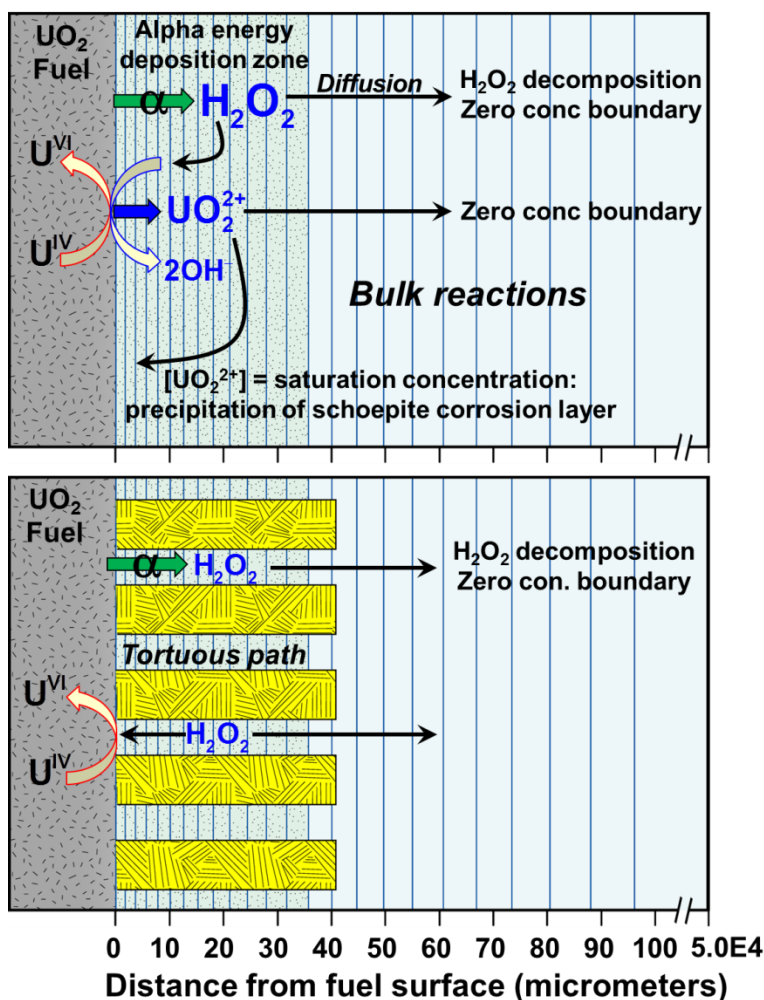


**Figure 3.1** Spatial diffusion grid for MPM showing individual calculation nodes as vertical lines and summarizing key processes accounted for by the model (top image). Note the logarithmic distribution of calculation points at the fuel/solution interface. The baseline number of individual calculation nodes for the MPM is 200 (not all shown); however, this number can be increased by the modeler if higher spatial resolution is required. The bottom image focuses on how the presence of a U(VI) corrosion layer can influence the fuel degradation rate by blocking

alpha energy from being deposited in solution and by moderating the diffusion of species towards and away from the reacting fuel surface.

Electrochemical rate expressions are used as boundary conditions for species that participate in the interfacial electrochemical reactions. These reactions, as well as key bulk reactions accounted for in the model are listed in Table 3.1.

**Table 3.1** Surface electrochemical reactions and bulk solution reactions tracked in the MPM.

<b>Reactions</b>	
<i>Anodic reactions at fuel surface</i>	
$\text{UO}_2 \rightarrow \text{UO}_2^{2+} + 2\text{e}^-$	
$\text{UO}_2 + 2\text{CO}_3^{2-} \rightarrow \text{UO}_2(\text{CO}_3)_2^{2-} + 2\text{e}^-$	
$\text{H}_2\text{O}_2 \rightarrow \text{O}_2 + 2\text{H}^+ + 2\text{e}^-$	
$\text{H}_2 \rightarrow 2\text{H}^+ + 2\text{e}^-$	
<i>Cathodic reactions at fuel surface</i>	
$\text{H}_2\text{O}_2 + 2\text{e}^- \rightarrow 2\text{OH}^-$	
$\text{O}_2 + 2\text{H}_2\text{O} + 4\text{e}^- \rightarrow 4\text{OH}^-$	
<i>Homogeneous Bulk Reactions</i>	
$\text{UO}_2^{2+} + 2\text{H}_2\text{O} \rightarrow \text{UO}_3 \cdot 2\text{H}_2\text{O} + 2\text{H}^+$	
$\text{UO}_2(\text{CO}_3)_2^{2-} + 2\text{H}_2\text{O} \rightarrow \text{UO}_3 \cdot \text{H}_2\text{O} + 2\text{CO}_3^{2-} + 2\text{H}^+$	
$\text{UO}_3 \cdot \text{H}_2\text{O} + 2\text{CO}_3^{2-} + 2\text{H}^+ \rightarrow \text{UO}_2(\text{CO}_3)_2^{2-} + 2\text{H}_2\text{O}$	
$\text{O}_2 + 2\text{H}_2\text{O} + 4\text{Fe}^{2+} \rightarrow 4\text{Fe(III)} + 4\text{OH}^-$	
$\text{H}_2\text{O}_2 + 2\text{Fe}^{2+} \rightarrow 2\text{Fe(III)} + 2\text{OH}^-$	
$\text{UO}_2^{2+} + \text{Fe}^{2+} \rightarrow \text{Fe(III)} + \text{U(IV)}$	
$\text{UO}_2(\text{CO}_3)_2^{2-} + \text{Fe}^{2+} \rightarrow \text{Fe(III)} + \text{U(IV)} + 2\text{CO}_3^{2-}$	
$\text{H}_2\text{O}_2 \rightarrow \text{H}_2\text{O} + 0.5\text{O}_2$	

The inclusion of alpha radiolysis in the MPM is essential because, at low concentrations of dissolved oxygen, the only oxidants within a repository system are radiolytic species (e.g., molecular hydrogen peroxide). The current model does not include the potential for peroxide complexes with  $\text{UO}_2^{2+}$ . Therefore, predicting an accurate rate of fuel matrix degradation in anoxic settings such as crystalline rock and clay/shale repository environments requires an accurate description of radiolysis.

Calculating the alpha dose rate (and thus  $\text{H}_2\text{O}_2$  concentration) for corroding  $\text{UO}_2$  fuel is complicated by the effects of U(VI) corrosion products (modeled as schoepite,  $[(\text{UO}_2)_8\text{O}_2(\text{OH})_{12}](\text{H}_2\text{O})_{12}$  in MPM). The U(VI) corrosion product layer has three effects on the

rate of fuel degradation predicted by the MPM:

- Slows rate of oxidative dissolution by decreasing the reactive surface area of the fuel (blocking or masking reaction sites).
- Slows rate of oxidative dissolution by blocking alpha-particles from interacting with water and producing radiolytic oxidants (decreases total moles  $H_2O_2$  produced near fuel surface). The magnitude of this effect is proportional to surface coverage of corrosion layer.
- Corrosion layer can slow the rate of oxidative dissolution by slowing the rate of diffusion of oxidants to the fuel surface: U(VI) layer is a tortuous porous mass of crystals (simulated in MPM by a parallel pores with constant tortuosity).

All three of these effects are modeled in the MPM by a radiolysis "sub-routine" that was recoded (for details see Jerden et al., 2013) from the original Canadian mixed potential model (King and Kolar, 1999). As in Canadian model, alpha-particles in the MPM are assumed to have a constant energy of 5.3 MeV and a solution penetration distance ( $\alpha_{PEN}$ ) of 35  $\mu m$ . The modeler can set the penetration distance over the range of  $\alpha_{PEN} = 45$  micrometers for  $\sim 6.0$  MeV alpha-particles down to  $\alpha_{PEN} = 10$   $\mu m$  for  $\sim 2.3$  MeV particles (King and Kolar, 1999). In the MPM, the default generation value for hydrogen peroxide produced by alpha-radiolysis is assumed to be  $1.021E-4$  mol/Gy/m<sup>3</sup> (Christensen and Sunder, 2000).

As stated above, the main objective of the current report is to present a strategy by which this simplified radiolysis "sub-routine" can be replaced by the more rigorous radiolysis model. To facilitate the discussion of this model integration effort, the geometry assumed for the MPM and the chemical processes that are taken into account are summarized below:

### User-defined inputs

- Length of model diffusion grid (fuel surface to environmental boundary, default is 5 millimeters)
- Number of calculation nodes (points) in diffusion grid (default is 200)
- Duration of simulation
- Surface coverage of fission product alloy phase

### Parameters

- Alpha-particle penetration depth
- Generation value for  $H_2O_2$  ( $G_{H_2O_2}$ ) (moles per alpha energy deposited per time). This will be replaced by the  $G_{i,cond}$  which is calculated and passed from the RM to the MPM (defined in section 2.3 above).
- Charge transfer coefficients
- Rate constants (*function of temperature*)
- Standard potentials (*function of temperature*)

- Diffusion coefficients (*function of temperature*)
- Saturation con. U(VI) (*function of temperature*)
- Activation energies for temperature dependencies
- Porosity of schoepite (corrosion) layer
- Tortuosity of schoepite (corrosion) layer
- Resistance between UO<sub>2</sub> and fission product alloy (epsilon) phase

### Constants (not explicit in model)

- pH of bulk solution nominally 9.5 (pH implicit in parameter values)
- Pressure (O<sub>2</sub>, H<sub>2</sub> are set and tracked as dissolved concentrations)

### Variables

- Dose rate
- Temperature
- Starting concentrations of oxidants and complexants: [O<sub>2</sub>], [CO<sub>3</sub><sup>2-</sup>], [H<sub>2</sub>], [Fe<sup>2+</sup>]

### Parameters Calculated by model (output)

- Corrosion potential
- Current densities for interfacial redox reactions
- Flux of species from fuel surface
- Concentrations of all species at each node (point) in diffusion grid after each time step
- Corrosion layer thickness

## 3.3 Mathematical Model

The mathematical approach for the MPM is described in detail in Jerden et al., 2012 and Jerden et al., 2013. The key aspects of the approach are how oxidants that cause fuel degradation are treated. The two oxidants currently included in the MPM are (1) hydrogen peroxide, which is formed by alpha radiolysis of water, and (2) oxygen, which has two sources: the initial amount in the environment (set by modeler) and an amount formed by the decomposition of hydrogen peroxide at the fuel surface and in the bulk solution. The mass balance equations that track hydrogen peroxide and oxygen are shown as Equations 3.1 and 3.2 (applied at every node within the 5 mm diffusion grid).

$$\varepsilon \frac{\partial C_{O_2}}{\partial t} = \frac{\partial}{\partial x} \left( \tau_f \varepsilon D_{O_2} \frac{\partial C_{O_2}}{\partial x} \right) - \varepsilon k_3 C_{O_2} C_{Fe^{2+}} \quad (3.1)$$

$$\varepsilon \frac{\partial C_{H_2O_2}}{\partial t} = \frac{\partial}{\partial x} \left( \tau_f \varepsilon D_{H_2O_2} \frac{\partial C_{H_2O_2}}{\partial x} \right) + \varepsilon G_{H_2O_2} R_D - \varepsilon k_4 C_{H_2O_2} C_{Fe^{2+}} \quad (3.2)$$

where  $\varepsilon$  is the porosity of the schoepite corrosion layer (default value is 45%),  $C_i$  is concentration of species  $i$  (moles/L),  $t$  is time (years),  $x$  is the horizontal distance along diffusion grid (micrometers),  $\tau$  is the tortuosity factor for pores in schoepite corrosion layer (default is 0.1),  $k_3$ ,  $k_4$  are the rate constants for the reduction of oxygen and hydrogen peroxide by aqueous ferrous iron by the reactions given in Equations (3.3) and (3.4),  $G_{H_2O_2}$  is the radiolytic generation value of hydrogen peroxide (moles/(J/kg)/seconds),  $R_D$  is dose rate (Gy/second). Similar mass balance equations exist for all species included in the MPM.



The thickness of the schoepite corrosion layer is determined by computing the integral of the mass per volume (moles/m<sup>3</sup>) of schoepite for every grid point and using the molecular weight, mineral density and porosity to determine the  $x$  dimension of the layer.

The rate of generation of hydrogen peroxide is determined by the generation factor in mol/(J/kg)/m<sup>3</sup> multiplied by the dose rate (J/kg) and the radiolysis cutoff distance [ $g(x)$ ] which is defined as the zone of solution irradiated by the fuel. In the current version of the MPM, the amount of energy absorbed by solution in the 35 micrometer irradiated zone is constant. The current model does not account for attenuation of the alpha particle energy away from the fuel surface, but this may be included with the RM.

### 3.3.1 Geometric Scale

The length of the logarithmic grid of the model diffusion cell is adjustable but has been set at 5 millimeters (as shown in Figure 3.1) for all of the sensitivity runs performed to date. The number of calculation points along the diffusion grid can also be set by the user. Based on the simulations with times greater than 1000 years we have performed to-day, 200 grid points provides a good balance between the amount of time required to run the model and the spatial resolution of component concentrations within the grid.

### 3.3.2 Time Scale

The magnitude of each time step is determined by the total simulation time and the number of temporal calculation points specified. Both of these values are set by the user. The time steps are spaced logarithmically, with the finer spacing at the beginning of the run. For simulation runs of 10000 years or more, optimal time steps range from 0.1 years early in the simulation to 1000 years towards the end of the simulation.

## 3.4 Example of MPM Calculations

Figure 3.2 shows examples of results from MPM simulations of reaction for ten thousand years with hydrogen peroxide generation values from  $1.0\text{E-}4$  moles/(J/kg)/m<sup>3</sup> (theoretical value from Christensen and Sunder, 2000) to  $1.0\text{E-}5$  moles/(J/kg)/m<sup>3</sup> (arbitrarily chosen to study model sensitivity). For this model run the temperature and dose rate within the model diffusion grid were held constant at 25°C and 0.1 Gy/s respectively, the initial oxygen concentration was  $1.0\text{E-}6$  moles/L and the background concentrations of carbonate, iron and hydrogen were set to zero.

To give a sense of the temporal resolution of the model for the default settings of 200 grid points and 100 time steps, results for each time step are shown as individual data points in Figure 3.2. The top plot shows that the rate of oxidative dissolution of the fuel decreases by a factor of approximately 2 due to the precipitation of the schoepite corrosion layer, which physically prevents alpha particles from irradiating the solution at the surface of the fuel. Because the corrosion layer is modeled as a set of uniform parallel pores, the amount of fuel area masked is determined by its porosity (default is 50%). The oxidative dissolution rate is also predicted to decrease by a factor of 8 due to this lower production rate of hydrogen peroxide from the order of magnitude decrease in the  $G_{\text{H}_2\text{O}_2}$ . The dissolution rate does not decrease further because the background concentration of oxygen supports oxidative dissolution of the fuel.

The middle diagram of Figure 3.2 shows the current densities for the dominant interfacial redox reactions. The kinetic balance of these cathodic and anodic reactions determines the corrosion potential from which the oxidative dissolution rate of the fuel is calculated. The bottom diagram shows the steady state diffusion profiles for hydrogen peroxide over the diffusion grid. This plot highlights the effect of the schoepite corrosion layer in both blocking alpha-particles emitted from the fuel from irradiating the solution and in moderating the diffusion to and from the reacting fuel surface.

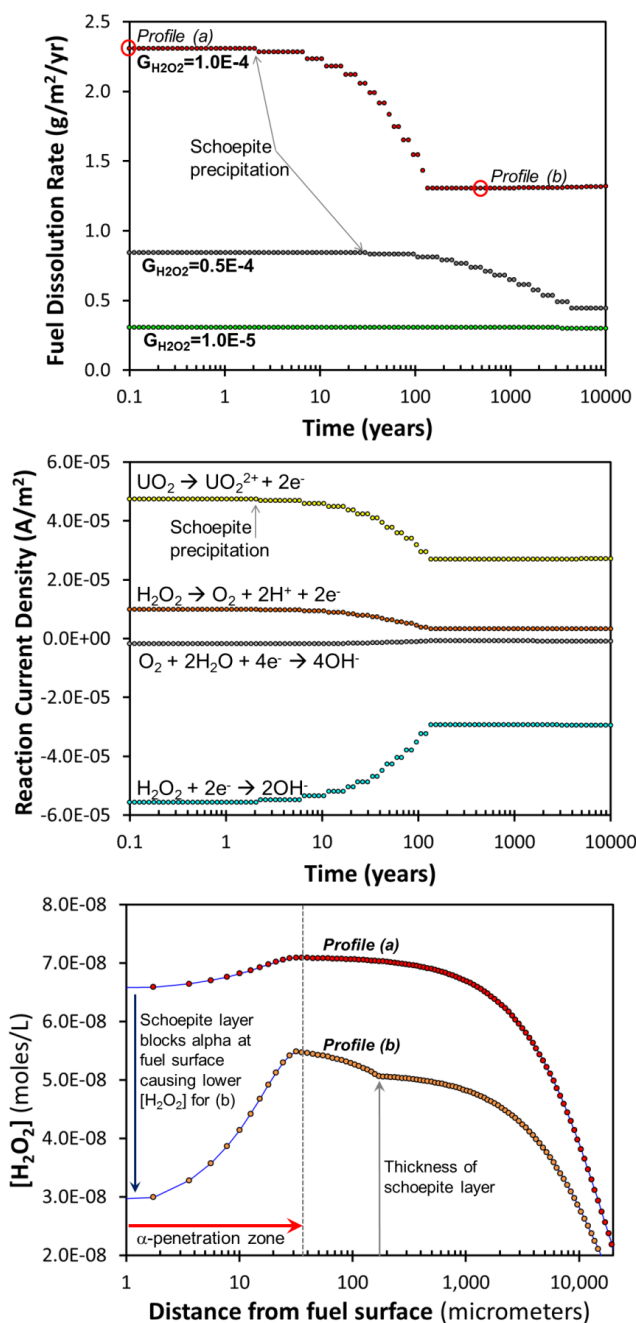


**Figure 3.2** Results from recent MPM runs investigating the sensitivity of fuel degradation rate to changes in the G-value for  $\text{H}_2\text{O}_2$  in mole/(J/kg)/second (top). Individual time steps are represented as single data points. The middle diagram shows the reaction current densities ( $G_{\text{H}_2\text{O}_2}=1.0\text{E-}5$ ) for the redox reactions that determine the fuel corrosion potential and fuel degradation rate. The bottom diagram shows  $\text{H}_2\text{O}_2$  concentration profiles for the two time steps identified in the top diagram.

## 4. COUPLING MPM/RM MODELS

Coupling the RM and MPM will provide a scientifically rigorous predictive tool for calculating the degradation rate of used fuel. By combining the models, we ensure that the fuel degradation calculations used to determine performance assessment source terms account for all major radiolytic, electrochemical and corrosion processes that can influence radionuclide release. The conceptual approach for coupling the RM and MPM is summarized in Figure 4.1. This diagram shows that the integrated Fuel degradation model consists of three modules:

- The *Radiolysis Module* (green box), which provides a rigorous treatment of chemical processes associated with the absorption of ionizing radiation near the surface of the exposed fuel. Supplies concentrations used to calculate fuel matrix degradation.
- The *Mixed Potential Module* (blue process boxes), which provides the rate of fuel matrix degradation (accounts for both oxidative and chemical dissolution).
- The *Instant Release Fraction*, which provides the masses of key radionuclides that will be released from the fuel promptly after the time of exposure (release rate is more rapid than predicted matrix degradation rate).

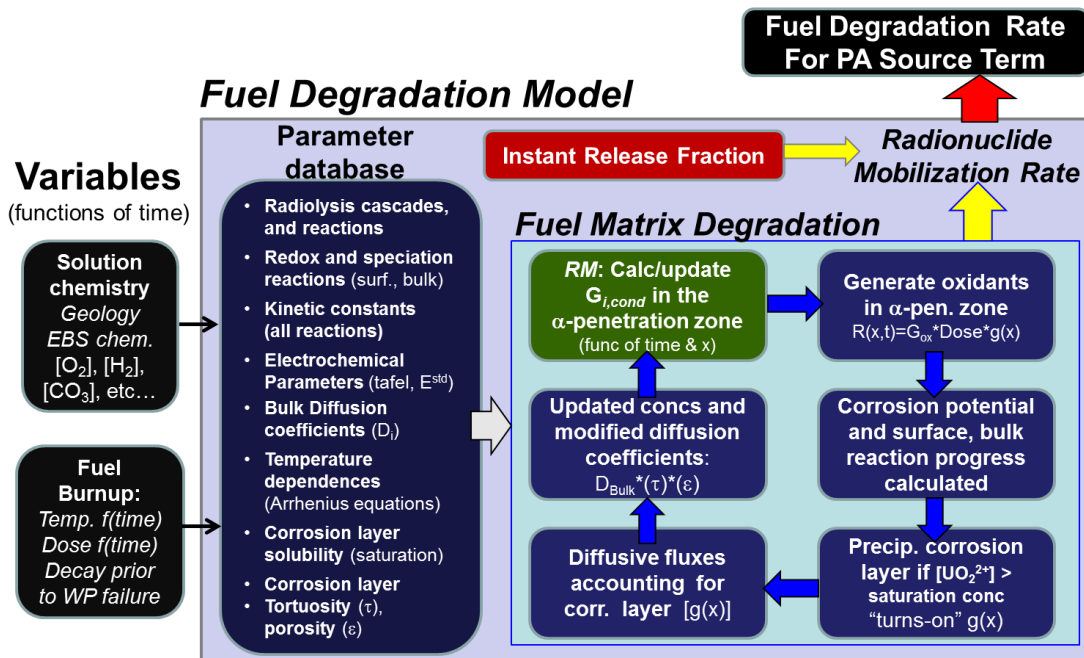


**Figure 4.1** Summary information flow diagram showing interfaces between fuel and site information, FDM (MPM shown by blue boxes, RM by green box, and IRF by red box), and PA.

The strategy for development and implementation of the integrated Fuel Degradation Model (FDM) involves the flow of information both to and from other performance assessment level models. As shown in Figure 4.1, required inputs to the FDM include quantitative descriptions of the composition of the groundwater/in-package solution in contact with the fuel as well as

information regarding the fuel being modeled, such as the changes in fuel temperature and dose rate with time. The temperature and dose information, which are directly used in the FDM, are determined by the fuel burn-up as well as the decay or cooling time elapsed prior to fuel exposure to environmental solutions (e.g., time before repository emplacement + time after emplacement before waste package failure).

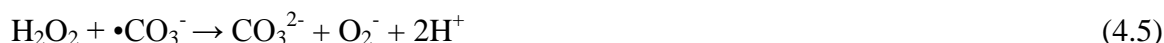
The initial conditions, temperature and dose rate functions will be combined with an extensive radiolysis-electrochemical-kinetic database and used by the FDM to produce a rate of fuel matrix degradation. The matrix degradation rate will be combined with inventory-specific instant release fraction calculation to yield a radionuclide mobilization rate source term on a per waste package basis for performance assessment calculations.

As shown in Figure 4.1, the key link between the RM and MPM is the conditional generation values for radiolytic species. Conditional generation values take into account the effects of shielding by alteration layers and chemical reactions in the evolving solution on the G values ( $G_{i,cond}$ ). Coupling of the models involves the passing of spatial solution concentrations from the MPM to the RM and then the conditional generation values for relevant species from the RM to the MPM for use in the next time step of the MPM (Figure 4.1). For this exchange to work, the spatial calculation grid within the alpha penetration zone must be identical in each model (currently 14 nodes within 35 micrometers of the alpha source).

#### 4.1 Parameter values provided by RM to MPM

The RM will provide conditional G-values for all oxidants capable of degrading the fuel (currently  $H_2O_2$  and  $O_2$ ) as well as hydrogen, which can protect the fuel from oxidative dissolution if its oxidation is catalyzed at the reacting surface. The conditional G-values will be supplied to the MPM for every calculation node located within the  $\alpha$ -particle penetration zone (currently 14 nodes over the 35  $\mu m$   $\alpha$ -particle penetration zone).

The conditional G-values calculated by the RM are more accurate than the theoretical  $G_{H_2O_2}$  used as a default in the MPM because the RM accounts for the diffusion of, and reactions between, intermediate radiolytic species such as  $e_{aq}^-$ ,  $\cdot H$ ,  $\cdot OH$ ,  $\cdot OH_2$ , and  $\cdot CO_3^-$ . Examples of reactions that can lead to a decreased yield of hydrogen peroxide relative to the amount predicted in the MPM are:



## 4.2 Parameter values provided by MPM to RM

For the RM to calculate an accurate description of the generation values for relevant radiolytic species (e.g.,  $\text{H}_2\text{O}_2$ ) it needs the following information from the MPM:

- Concentrations of species that are radiolytically active (e.g., species such as  $\text{CO}_3^{2-}$  or  $\text{Cl}^-$  that produce reaction cascades when excited) or otherwise interact with radiolytic species (e.g.,  $\text{O}_2$ ,  $\text{H}_2$ ,  $\text{Fe}^{\text{II}}$ ).
- The modified diffusion coefficients for all relevant species (e.g.,  $\text{O}_2$ ,  $\text{H}_2$ ,  $\text{Fe}^{\text{II}}$ ,  $\text{CO}_3^{2-}$ ) at all calculation nodes present within the tortuous corrosion layer (see Figure 2 for visual explanation of assumed corrosion product geometry)

### Matching/partitioning physical, chemical, radiolytic processes

Physical, chemical and radiolytic processes will be matched by ensuring that the same spatial diffusion grid is used for both models. Diffusion depends on the spatial dimension of the grid, so a uniform 5 millimeter linear distance will be used for both models as a default; however, this value can be altered by the modeler. To ensure that the chemical and radiolytic processes match both models will contain the same number, and spacing of calculation nodes within the alpha penetration zone (default is 14 nodes). The key time and space dependent variables dose rate and temperature will also be matched in the two models.

### Coordinating time scales

The RM calculations that produce the conditional G-values require short time steps relative to the MPM (kinetics on order of seconds). Therefore, the two models will not be time synchronized. Rather the RM will be run independently and the resulting conditional G-values will be handed off at a specific time point during a MPM simulation. There are three options for timing this hand-off:

- Option: Use RM to provide conditional G-value at each time step in MPM
- Option: Use RM to provide conditional G-value after a constant number of time steps in MPM
- Option: Use the RM to identify solution concentrations that have significant impact on  $[\text{H}_2\text{O}_2]$  and conditional G-value

The best option in terms of model fidelity is for the RM to provide the conditional G-values at the beginning of each MPM time step. This will be the option pursued as we move forward with implementation of the coupled model.

### Conditional G-factor

$G_{\text{cond}}$  is defined as the steady state generation value (moles of species (i) per alpha energy deposited) averaged over the 35 micrometer alpha penetration depth adjacent to the fuel surface.

The  $G_{\text{cond}}$  value is generated from Equation 2.3 for feeding into the MPM. The conditional  $G$ -value is dependent on the solution conditions and environment.

To accurately calculate  $G_{\text{cond}}$  for a solution generated by a given number of MPM time steps, the RM will need the following information:

- Dose rate.
- Temperature.
- Concentrations of reactive species  $[\text{O}_2]$ ,  $[\text{H}_2]$ ,  $[\text{CO}_3^{2-}]$ , and for application to other generic forms of geologic repository, terms for  $[\text{Cl}^-]$ ,  $[\text{Br}^-]$ ,  $[\text{SO}_4^{2-}]$ , and others will become important.
- Diffusion coefficients of relevant species at the last MPM step (these change in alpha penetration zone when a corrosion layer is present due to tortuosity factor.)
- Thickness of corrosion layer.

The dose rate and temperature are characteristics of the fuel and disposal system, and the other values are calculated or tracked in MPM. All are handed off to RM whenever it is determined that a new  $G_{\text{cond}}$  is needed for the next time step of the MPM run. The need for a new  $G_{\text{cond}}$  could be triggered by concentration thresholds determined to result in significant changes in the  $G$ -values from previous sensitivity runs (e.g., sets of  $\text{H}_2$  and  $\text{O}_2$  concentrations that favor the rapid decomposition of  $\text{H}_2\text{O}_2$ ) (see Figure 2.3 and 2.4).

### 4.3 Interface Approaches

Several options being considered for coupling the RM and MPM are listed below. Different options have advantages and disadvantages based on the extent of coding that would be required and the ease of use of the final product.

**Option 1:** Add radiolysis module as subroutine within mixed potential module code. This would involve re-coding the RM from Fortran into MATLAB or alternatively recoding the MPM into Fortran so that the two models would run as part of the same program.

- Pros: full RM code included in integrated model, not limited to abstracted form of the RM, seamless transfer of information.
- Cons: relatively large amount of time and effort required to support recoding.

**Option 2:** Represent radiolysis module as an analytical expression within mixed potential module code. This would involve minimal coding in MATLAB, but would require significant effort to define an analytical form that captures the full range of conditional dependencies accounted for in the RM.

- Pros: coding work is streamlined and simplified, seamless transfer of information.

- Cons: uncertainty of success of approach, it is not clear that a single analytical expression can capture all of the relevant conditional dependencies accounted for in the full RM.

**Option 3:** Provide radiolysis module results as look-up table of conditional generation values produced by running the RM over the full range of relevant conditions. This G-value look-up table would be treated by the MPM as part of the parameter database.

- Pros: no coding work needed, seamless transfer of information.
- Cons: relatively large amount of time and effort to produce exhaustive table that considers all relevant conditions,

**Option 4:** Maintain radiolysis model and mixed potential module as separate codes that call each other during a fuel degradation model run.

- Pros: no coding work needed, not limited to abstracted version of the RM.
- Cons: uncertainty of success of approach, it is not clear that the Fortran and MATLAB codes and pass the needed information back and forth as they currently exist. Even if possible this approach may dramatically increase computing time needed to run the FDM.

## 5. Conclusions

The  $G_{\text{cond}}$  is calculated in the RM and handed off to the MPM, where it is used to calculate the spatial generation of  $[\text{H}_2\text{O}_2]$  from the dose rate as affected by surface reactions with the fuel and diffusion.  $G_{\text{cond}}$  is defined as the steady state generation value (moles of species (*i*) per alpha energy deposited) averaged over the 35  $\mu\text{m}$  alpha penetration depth adjacent to the fuel surface. It is useful though not entirely necessary that the total deposition depths are the same in the RM and MPM, and it may be valuable that they be discretized the same. This is because the  $\text{H}_2\text{O}_2$  concentration is calculated at much shorter time scales within the RM compared to the MPM. When using the discretized case of the RM,  $G_{\text{cond}}$  becomes proportional to the diffusive flux of species (*i*) exiting the alpha penetration zone.

The coupling of the RM and MPM requires running the models separately because the MPM uses time steps on the order of years, while the RM uses time steps on the order of seconds. An alternative to actively linking the RM and MPM is to develop an analytic expression that determines  $G_{\text{cond}}$  for a given set of conditions. The analytic expression would be coded directly into MATLAB and run with the MPM. However, this does not establish a true working link and the full capabilities of RM would be lost. Furthermore, the determination of analytical expressions for the full ranges of environments may prove to be onerous.

Currently the only radiolytic species in the MPM is  $\text{H}_2\text{O}_2$ . Other radiolytic species will need to be added to the MPM for it to be applicable to the full range of relevant geologic and EBS environments. The radiolytic species that need to be added can be determined by sensitivity runs using the RM for the range of relevant solution compositions for sites of interest. The focus of RM sensitivity runs should be on radiolytically active species (for example:  $\text{Cl}^-$ ,  $\text{Br}^-$ ,  $\text{NO}_3^-$ ,  $\text{CO}_3^{2-}$ ,  $\text{SO}_4^{2-}$ ) and should determine concentration thresholds above which radiolytic species other than  $\text{H}_2\text{O}_2$  significantly impact fuel oxidation become important.

### **Argonne Acknowledgment**

Government License Notice: The submitted manuscript has been created by UChicago Argonne, LLC, Operator of Argonne National Laboratory (“Argonne”). Argonne, a U.S. Department of Energy Office of Science laboratory, is operated under Contract No. DE-AC02-06CH11357. The U.S. Government retains for itself, and others acting on its behalf, a paid-up nonexclusive, irrevocable worldwide license in said article to reproduce, prepare derivative works, distribute copies to the public, and perform publicly and display publicly, by or on behalf of the Government. This work was supported by the U.S. Department of Energy, Office of Nuclear Energy, under Contract DE-AC02-06CH11357.

### **Pacific Northwest National Laboratory Acknowledgment**

This work was supported by the US Department of Energy, Office of Nuclear Energy, Used Fuel Disposition (UFD) – Repository Science (RS) Program under Contract. Pacific Northwest National Laboratory is operated for the U.S. Department of Energy by Battelle under Contract DE-AC05-76RL01830.

## 6. References

Christensen, H., Sunder, S. (1996) An evaluation of water layer thickness effective in oxidation of  $UO_2$  fuel due to radiolysis of water, *Journal of Nuclear Materials* 238: 70-77.

Freeze, G., Mariner, P., Houseworth, J., Cunnane, J., and F. Caporuscio, F. (2010). *Used Fuel Disposition Campaign Features, Events, and Processes (FEPs): FY10 Progress Report*, August 2010.

Jerden, J., Frey, K., Cruse, T., and Ebert, W. (2012). *Waste Form Degradation Model Status Report: Electrochemical Model for Used Fuel Matrix Degradation Rate*. FCRD-UFD-2012-000169.

Jerden, J., Frey, K., Cruse, T., and Ebert, W. (2013). *Waste Form Degradation Model Status Report: ANL Mixed Potential Model, Version 1. Archive*. FCRD-UFD-2013-000057.

King, F. and Kolar, M. (1999) *Mathematical Implementation of the Mixed-Potential Model of Fuel Dissolution Model Version MPM-V1.0*, Ontario Hydro, Nuclear Waste Management Division Report No. 06819-REP-01200-10005 R00.

King, F. and Kolar, M. (2002) *Validation of the Mixed-Potential Model for Used Fuel Dissolution Against Experimental Data*, Ontario Hydro, Nuclear Waste Management Division Report No. 06819-REP-01200-10077-R00.

King, F. and Kolar, M. (2003) *The Mixed-Potential Model for  $UO_2$  Dissolution MPM Versions V1.3 and V1.4*, Ontario Hydro, Nuclear Waste Management Division Report No. 06819-REP-01200-10104 R00.

Pastina, B. and LaVerne, J. A. (2001) Effect of Molecular Hydrogen on Hydrogen Peroxide in Water Radiolysis, *Journal of Physical Chemistry* A105: 9316-9322.

Poinsot, C. Ferry, C. M. Kelm, B. Grambow, A. Martinez, A., Johnson, L., Andriamoolona, Z., Bruno, J., Cachoir, C., Cavedon, J.M., Christensen, H., Corbel, C., Jegou, C., Lemmens, K., Loida, A., Lovera, P., Miserque, F. de Pablo, J., Poulesquen, A., Quinones, J. Rondinella, V., Spahiu, K., and D. H. Wegen, (2004) *Spent Fuel Stability under Repository Conditions: Final Report of the European Project*, European Commission, 5<sup>th</sup> EURATOM FRAMEWORK PROGRAMME, 1998-2002.

Radulescu, G. (2011) *Radiation Transport Evaluations for Repository Science*, ORNL/LTR-2011/294, LETTER REPORT, Oak Ridge National Laboratory, August, 2011.

Sassani et al., 2012 *Integration of EBS Models with Generic Disposal System Models*, U.S. Department of Energy, Used Fuel Disposition Campaign milestone report: M2FT-12SN0806062, September, 7 2012

Shoesmith, D.W., Kolar, M., and King, F. (2003). A Mixed-Potential Model to Predict Fuel (Uranium Dioxide) Corrosion Within a Failed Nuclear Waste Container, *Corrosion*, 59, 802-816.

Wittman, R. S. and Buck, E. C. (2012) Sensitivity of  $\text{UO}_2$  stability in a reducing environment on radiolysis model parameters, *Materials Research Society Proceedings Symposium*, 1444, 3-8.